Optics Communications 424 (2018) 44–47

Contents lists available at ScienceDirect

Optics Communications

journal homepage: www.elsevier.com/locate/optcom

Dynamics in a saturable nonlinear waveguide coupler

J.D. Huerta Morales

Instituto Nacional de Astrofísica, Óptica y Electrónica, Calle Luis Enrique Erro No. 1, Sta. Ma. Tonantzintla, Puebla, CP 72840, Mexico

ARTICLE INFO

Keywords:
Optical waveguide couplers
Non-Hermitian dimer
Nonlinear optics
Classical physics

ABSTRACT

We study the propagation of electromagnetic field through a two-waveguide coupler with saturable nonlinearity. We show that the model supports an analytical solution for the dynamics, by means of the linearization of the system around fixed points. Also we prove that this model is isomorphic to the semi-classical non-Hermitian Bose–Hubbard dimer.

1. Introduction

Linear and nonlinear photonic lattices, optical systems composed of coupled waveguides, have been extensively explored for controlling light propagation [1–3]. Interestingly, coupling mode theory, the standard formalism to describe these systems, provides us with a structure similar to the discrete Schrödinger equation without the restriction of Hermiticity. For example, photonic lattices showing effective dynamics equivalent to parity-time symmetry [4,5]. Hence, optical systems have provided a platform to simulate $\mathcal{PT}$-symmetry models [6,7], which have been shown theoretically [8,9] and experimentally [10,11]. In particular, the standard $\mathcal{PT}$-symmetric optical coupler consists of two coupled waveguides with balanced effective gain and loss. Such dimers have been widely studied [12–14] including linear [15] and nonlinear mediums [16,17].

The standard nonlinear $\mathcal{PT}$-symmetric dimer has been analyzed in detail [18,19]. The two complex field amplitudes propagating through the dimer are governed by the evolution equations:

$$\begin{aligned} -i\partial_z E_1 &= i\gamma E_1 + E_2 + \kappa |E_1|^2 E_1, \\ -i\partial_z E_2 &= -i\gamma E_2 + E_1 + \kappa |E_2|^2 E_2, \end{aligned} \tag{1}$$

with κ the nonlinearity coefficient and γ the gain–loss parameter. The study of this type of dimers provides the basis for the development of optical devices such as nonlinear directional couplers useful for the control of optical signals [20,21], power-sensitive switches and polarization beam splitters [22]. Recently a general model for non-Hermitian nonlinear dimer coupling has been solved considering saturable nonlinearity [23], giving rise to the use of fiber amplifiers and design of polarization rotators.

In this paper, we will show that considering saturable nonlinearity and renormalized fields, leads to an optical analogy of the semi-classical non-Hermitian Bose–Hubbard dimer [24], showing three dynamic regions that we will discuss in detail.

E-mail address: jd_huerta@inaoep.mx.

2. Model

We will consider the coupled-mode approach to describe the propagation of electromagnetic field through two coupled waveguides:

$$\begin{aligned} -i\partial_z E_1 &= \left(\beta_{R1} + i\beta_{I1}\right) E_1 + g E_2 + \kappa_1 \frac{|E_1|^2}{|E_1|^2 + |E_2|^2} E_1, \\ -i\partial_z E_2 &= \left(\beta_{R2} + i\beta_{I2}\right) E_2 + g E_1 + \kappa_2 \frac{|E_2|^2}{|E_1|^2 + |E_2|^2} E_2, \end{aligned} \tag{2}$$

where we have considered the complex field amplitudes $E_j \equiv E_j(z)$ with $j = 1, 2$, and the renormalization of the nonlinear fields. The notation ∂_z to represent the partial derivative with respect to z. The imaginary part of the complex effective propagation constants, $\beta_j = \beta_{Rj} + i\beta_{Ij}$, are related to the gain–loss of each waveguide. The effective Kerr nonlinearity parameters and the effective coupling between the waveguides are, κ_j and g, respectively.

Let us instantaneously renormalize the field amplitudes,

$$\mathcal{E}_j = \frac{e^{-i\beta_0 z} E_j}{\sqrt{|E_1|^2 + |E_2|^2}}, \tag{3}$$

such that $|\mathcal{E}_1|^2 + |\mathcal{E}_2|^2 = 1$ at any given propagation distance. Note that we have introduced a phase and scaling factor to subtract the dynamics induced by the mean propagation constant, $\beta_0 = (\beta_1 + \beta_2)/2$. We can also scale the propagation distance by the coupling parameter, gz, and consider equal Kerr nonlinearities in order to recover a non-Hermitian, nonlinear dimer,

$$\begin{aligned} -i\partial_z \mathcal{E}_1 &= \mathcal{E}_2 + \left[\beta_R + \kappa|\mathcal{E}_1|^2 + 2i\beta_I|\mathcal{E}_2|^2\right]\mathcal{E}_1, \\ -i\partial_z \mathcal{E}_2 &= \mathcal{E}_1 - \left[\beta_R - \kappa|\mathcal{E}_2|^2 + 2i\beta_I|\mathcal{E}_1|^2\right]\mathcal{E}_2, \end{aligned} \tag{4}$$

https://doi.org/10.1016/j.optcom.2018.04.036
Received 18 February 2018; Received in revised form 11 April 2018; Accepted 13 April 2018

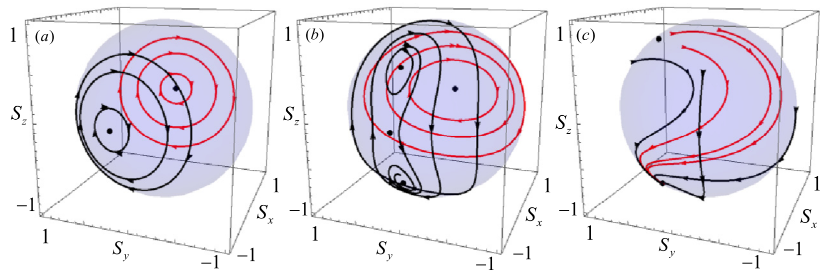

Fig. 1. Dynamical of the system on the Poincaré sphere: (a) RI, $|\beta_I| < 1$ and $|\kappa| < 2$, (b) RII, $|\beta_I| < 1$ and $|\kappa| \geq 2$, (c) RIII, $|\beta_I| \geq 1$ and for any value of κ.

where we have defined a scaled Kerr parameter $\kappa = \kappa_j/g$ with $\kappa_1 = \kappa_2$, and real auxiliary variables, $\beta_R = (\beta_{R1} - \beta_{R2})/(2g)$ and $\beta_I = (\beta_{I1} - \beta_{I2})/(2g)$. Thus, this model has an underlying dynamics equivalent to a dimer with a standard self-modulated nonlinearity and a non-Hermitian cross-modulated non-linearity that, in other circumstances, might appear un-physical.

In order to recover more information, we can follow the standard approach for the $\mathcal{PT}$-symmetric dimer [13,18,23] and define a Stokes-like vector, $\mathbf{S}_0 = (S_x, S_y, S_z)$, with components,

$$S_x = \mathcal{E}_1\mathcal{E}_2^* + \mathcal{E}_1^*\mathcal{E}_2,$$
$$S_y = i\left(\mathcal{E}_1\mathcal{E}_2^* - \mathcal{E}_1^*\mathcal{E}_2\right),$$
$$S_z = |\mathcal{E}_1|^2 - |\mathcal{E}_2|^2. \tag{5}$$

The norm of this vector will be a constant of motion, $S_0 = \sqrt{S_x^2 + S_y^2 + S_z^2} = |\mathcal{E}_1|^2 + |\mathcal{E}_2|^2 = 1$. The equations of motion for the vector components are straightforward to calculate,

$$F_x \equiv \partial_z S_x = \left[2\beta_I S_x + \kappa S_y\right] S_z + 2\beta_R S_y,$$
$$F_y \equiv \partial_z S_y = \left[2 + 2\beta_I S_y - \kappa S_x\right] S_z - 2\beta_R S_x,$$
$$F_z \equiv \partial_z S_z = -2S_y - 2\beta_I\left(1 - S_z^2\right), \tag{6}$$

and allow us to draw an analogy with the equations of motion for the non-Hermitian Bose–Hubbard dimer in the semi-classical limit, that is, for an infinitely large number of excitations in the model [24]. From these equations of motion, we can calculate the fixed points of the system. For the sake of understanding, we will present the four possible fixed points where the real part of propagation constant for waveguides are equal, $\beta_R = 0$,

$$\mathbf{S}_1 = \left(\sqrt{1-\beta_I^2}, -\beta_I, 0\right),$$
$$\mathbf{S}_2 = \left(-\sqrt{1-\beta_I^2}, -\beta_I, 0\right),$$
$$\mathbf{S}_3 = \left(\frac{2\kappa}{4\beta_I^2+\kappa^2}, -\frac{4\beta_I}{4\beta_I^2+\kappa^2}, \sqrt{\frac{4\beta_I^2+\kappa^2-4}{4\beta_I^2+\kappa^2}}\right),$$
$$\mathbf{S}_4 = \left(\frac{2\kappa}{4\beta_I^2+\kappa^2}, -\frac{4\beta_I}{4\beta_I^2+\kappa^2}, -\sqrt{\frac{4\beta_I^2+\kappa^2-4}{4\beta_I^2+\kappa^2}}\right). \tag{7}$$

Where some of these fixed points become imaginary, we can define three regions. Region I occurs when the absolute value of the scaled gain is less than the unit, $|\beta_I| < 1$, and the absolute value of the scaled Kerr nonlinearity is less than two, $|\kappa| < 2$. Here, the system has two fixed points, $\mathbf{S}_1$ and $\mathbf{S}_2$. Region II has four fixed points, $\mathbf{S}_1$ to $\mathbf{S}_4$, defined in the parameter range, $|\beta_I| < 1$ and $|\kappa| \geq 2$. Finally, region III occupies the rest of parameter space, $|\beta_I| \geq 1$ for all values of scaled Kerr nonlinearity, and has two fixed points, $\mathbf{S}_3$ and $\mathbf{S}_4$.

Table 1
Fixed point classification after linearization.

	RI $|\beta_I| < 1$ $|\kappa| < 2$	RII $|\beta_I| < 1$ $|\kappa| \geq 2$	RIII $|\beta_I| \geq 1$
$\mathbf{S}_1$	Center	Saddle point	
$\mathbf{S}_2$	Center	Center	
$\mathbf{S}_3$		Unstable focus	Unstable focus
$\mathbf{S}_4$		Stable focus	Stable focus

Table 2
Fixed point classification for particular cases.

	RII $|\beta_I| = 0$ $|\kappa| \geq 2$	RIII $|\beta_I| \geq 1$ $|\kappa| = 0$
$\mathbf{S}_1$	Saddle point	
$\mathbf{S}_2$	Center	
$\mathbf{S}_3$	Center	Unstable node
$\mathbf{S}_4$	Center	Stable node

3. System dynamics

In order to gather information of the dynamics, we can analyze the eigenvalues of the Jacobian matrix,

$$J = \begin{bmatrix} \frac{\partial F_x}{\partial S_x} & \frac{\partial F_x}{\partial S_y} & \frac{\partial F_x}{\partial S_z} \\ \frac{\partial F_y}{\partial S_x} & \frac{\partial F_y}{\partial S_y} & \frac{\partial F_y}{\partial S_z} \\ \frac{\partial F_z}{\partial S_x} & \frac{\partial F_z}{\partial S_y} & \frac{\partial F_z}{\partial S_z} \end{bmatrix}, \tag{8}$$

at the fixed points [25,26]. In region I, for each fixed point, $\mathbf{S}_1$ and $\mathbf{S}_2$, an eigenvalue is zero and the other two are complex with the real part equal to zero, then both are centers. In region II, the fixed point $\mathbf{S}_1$ is a saddle point, its eigenvalues are real with at least one positive and one negative, $\mathbf{S}_2$ is a center, $\mathbf{S}_3$ is unstable focus, a source, and $\mathbf{S}_4$ is stable focus, a sink. Finally, in region III, the fixed point $\mathbf{S}_3$ is unstable focus, the eigenvalues of its Jacobian are complex with positive real part, and $\mathbf{S}_4$ is stable focus, its corresponding eigenvalues are complex with negative real part. Table 1 summarizes these results and in Fig. 1 we observe the dynamics.

In the particular case, $\beta_I = 0$. The region I remains unchanged, in the region II the unstable focus $\mathbf{S}_3$ and stable focus $\mathbf{S}_4$, become centers, see Fig. 2(a); finally for region III, $\beta_I = 0$ is not allowed. We can see these results in Table 2. On the other hand, for $\kappa = 0$. The region I is the same, the region II does not allow the value $\kappa = 0$, and in the region III, Fig. 2(b), the fixed points unstable and stable focus become unstable and stable nodes, respectively. Now, the eigenvalues are real greater than zero and less than zero, in that order. Table 2 summarizes these results.

Fig. 1(a) presents a parameter region where only two fixed points exist, they are centers around which stable orbits exists. This shows that the system is integrable observing periodic closed trajectories, that